

Boise State University

ScholarWorks

Electrical and Computer Engineering Faculty
Publications and Presentations

Department of Electrical and Computer
Engineering

11-2023

Effect of Ultraviolet Light on Field Emission Performance and Lifetime of Lateral Field Emitter Devices

Ranajoy Bhattacharya
Boise State University

Marco Turchetti
Massachusetts Institute of Technology

Matthew Yeung
Massachusetts Institute of Technology

P. Donald Keathley
Massachusetts Institute of Technology

Karl K. Berggren
Massachusetts Institute of Technology

See next page for additional authors

This article may be downloaded for personal use only. Any other use requires prior permission of the author and AIP Publishing. This article appeared in:
Bhattacharya, R., Turchetti, M., Yeung, M., Keathley, P.D., Berggren, K.K., & Browning, J. (2023). Effect of Ultraviolet Light on Field Emission Performance and Lifetime of Lateral Field Emitter Devices. *Journal of Vacuum Science & Technology B*, 41(6), 063202,
and may be found at <https://doi.org/10.1116/6.0003142>.

Authors

Ranajoy Bhattacharya, Marco Turchetti, Matthew Yeung, P. Donald Keathley, Karl K. Berggren, and Jim Browning

Effect of ultraviolet light on field emission performance and lifetime of lateral field emitter devices

Cite as: J. Vac. Sci. Technol. B 41, 063202 (2023); doi: 10.1116/6.0003142

Submitted: 14 September 2023 · Accepted: 31 October 2023 ·

Published Online: 11 December 2023



Ranajoy Bhattacharya,¹  Marco Turchetti,²  Matthew Yeung,² P. Donald Keathley,²  Karl K. Berggren,² 
and Jim Browning^{1,a)} 

AFFILIATIONS

¹Department of Electrical and Computer Engineering, Boise State University, 1375 W University Dr., Boise, Idaho 83725

²Department of Electrical Engineering and Computer Science, Massachusetts Institute of Technology, 77 Massachusetts Ave., Cambridge, Massachusetts 02139

^{a)}Author to whom correspondence should be addressed: jimbrowning@boisestate.edu

ABSTRACT

Lateral field emission devices have been characterized before and after ultraviolet (UV) light exposure. Two types of planar device structures, diode and bowtie, were studied. These nanoscale devices have 9–15 nm tip-to-tip (bowtie) or tip-to-collector (diode) dimensions with the tips fabricated from Au/Ti. Typical currents of 2–5 nA per tip at 6 V were measured. It was observed that after UV exposure, the collected current was reduced by >28% for the case of a bowtie device; whereas the current was reduced by >39% for the case of a diode device. This reduction can be attributed to water vapor desorption on the dielectric surface between the structures, which in turn reduces surface leakage. The Fowler–Nordheim plot showed a straighter line after UV exposure. After the I–V test, the UV-exposed devices were placed on lifetime tests in a vacuum of $<10^{-8}$ Torr and were biased at 5 V DC. After 2600 h, an abrupt current decrease was observed: ~25% for the case of the bowtie and ~28% for the case of the diode device. Scanning electron microscope images of the bowtie and diode devices showed damage to the tips.

Published under an exclusive license by the AVS. <https://doi.org/10.1116/6.0003142>

I. INTRODUCTION

Planar field emitter devices such as bowtie and diode types are being studied as stable, longer lifetime sources of electrons for different types of applications, such as very high-frequency optical electronics,¹ surface plasmonic resonators using femtosecond pulse,^{2–5} and nano vacuum channel transistors (NVCTs).^{6,7} NVCTs that have ballistic electron transport in vacuum can have low energy loss, high operating temperature (>400 °C),^{8,9} high operating frequency, and radiation insusceptibility.^{7,8} Vacuum nano and microelectronic devices can have a variety of applications, such as sensors,¹⁰ field emission displays,¹¹ and high-performance integrated circuits (ICs).¹² Only a few practical applications of NVCTs in circuits were reported previously in spite of the fact that conceptual work and modeling of vacuum device based integrated circuits have been studied.^{13,14} For practical IC device implementation, NVCTs have to be improved in terms of reliability and stability. A previous study¹² carried out using a nanodiamond field emitter has shown a successful implementation

into differential amplifiers as an example of NVCT-based circuits, which advocate practical and reliable applications of planar NVCT devices. Planar field emission devices⁴ fabricated of Au/Ti metal with low turn-on voltage and stable field emission current have been studied, which can be implemented into high-frequency, NVCT devices.

Despite the impressive field emission performance from such lateral field emitters, a primary concern is the dominant collector current: from field emission or surface leakage. Lifetime and reliability are also other significant aspects. While a remarkable advancement in the lifetime and reliability of field emitters used in display devices were obtained in the early 1990s, only a few of these improvements¹⁵ were reported. Hence, information on field emission reliability and degradation is deficient, particularly for micro- and nanoscale structures.

The surfaces between the emitters and the gate are normally covered with adsorbates from air exposure, primarily water

vapor,^{16,17} which creates a conducting path between those electrodes, thus inducing a leakage current. The two goals of this work are to study the relative ratio of surface leakage to emission current and to characterize the long-term field emission and stability performance of the bowtie and diode structures.⁴ Surface leakage¹⁸ could be reduced by desorbing water vapor. Desorption of water vapor can be achieved by several methods including heating⁹ and UV exposure.^{19,20} However, the low temperature co-fired ceramic (LTCC) fixture used to mount and wire bond the die contains a silver paste that is not compatible at $>300\text{ }^{\circ}\text{C}$ in vacuum. As our prior work has clearly shown that UV exposure matches the water desorption effects of bakeout, a UV-based water desorption method was opted for this work. UV-based water desorption is a well-known method in vacuum systems to desorb.²⁰ The fabrication method of these devices are described in Sec. II. Experimental setup including the lifetime test system and test procedure are described in Sec. III, followed by device characterization data and lifetime test data in Sec. IV, and failure analysis data in Sec. V.

II. LATERAL DEVICE FABRICATION

The planar field emitters (bowtie and diode) were fabricated using a combination of electron beam lithography and etching, and a thorough fabrication process can be found elsewhere.⁴ Two device types (Au coated Ti), bowtie and diode, were characterized in this work. Scanning electron microscope (SEM) image of a diode [Fig. 1(a)] and a bowtie [Fig. 1(b)] device shows an emitter to collector gap of 9–15 nm. The primary dimension of the emitter structures is $\approx 100\text{ nm}$ narrowing down to sharp tips with radii $<10\text{ nm}$. Both structures had a variation in gap sizes due to the variation in the fabrication process. Also, the lack of a ballast resistor²¹ usually increases the probability of arcs,^{22–24} which in turn elevates the probability of tip failure. Note that these devices are single structures as opposed to large arrays, where the probability of failure in an array is much higher than for a single structure.

A section of the wafer was cut out after fabrication and attached to a low-temperature cofired ceramic (LTCC) test jig where the connection pads from the wafer section were wire bonded to the pads of the test jig. The pads of the test jig were internally connected to a multiwire ribbon cable. For characterization, the jig was placed inside a high vacuum test chamber. A photograph of the jig with the test die is shown in Fig. 1(c).

III. DEVICE CHARACTERIZATION SETUP

For UV exposure characterization and lifetime studies, two different test chambers were used. UV-exposed I-V sweeps were performed in a characterization test chamber. A detailed test chamber description can be found elsewhere.¹⁵ Up to a 6 V DC sweep was applied to the collector terminal where the emitter was kept at ground for the diode structure. For the bowtie structure, one terminal was kept at ground, whereas the other terminal was swept up to 6 V DC. Also, a reverse bias experiment was carried out on both devices. An RBD Instrument UV light (Model-MiniZ, wavelength = 185 nm, power = $350\text{ }\mu\text{W}/\text{cm}^2$) attached to the test chamber was used for the UV light exposure test. This UV light system has a fixed power supply, which did not allow us to observe

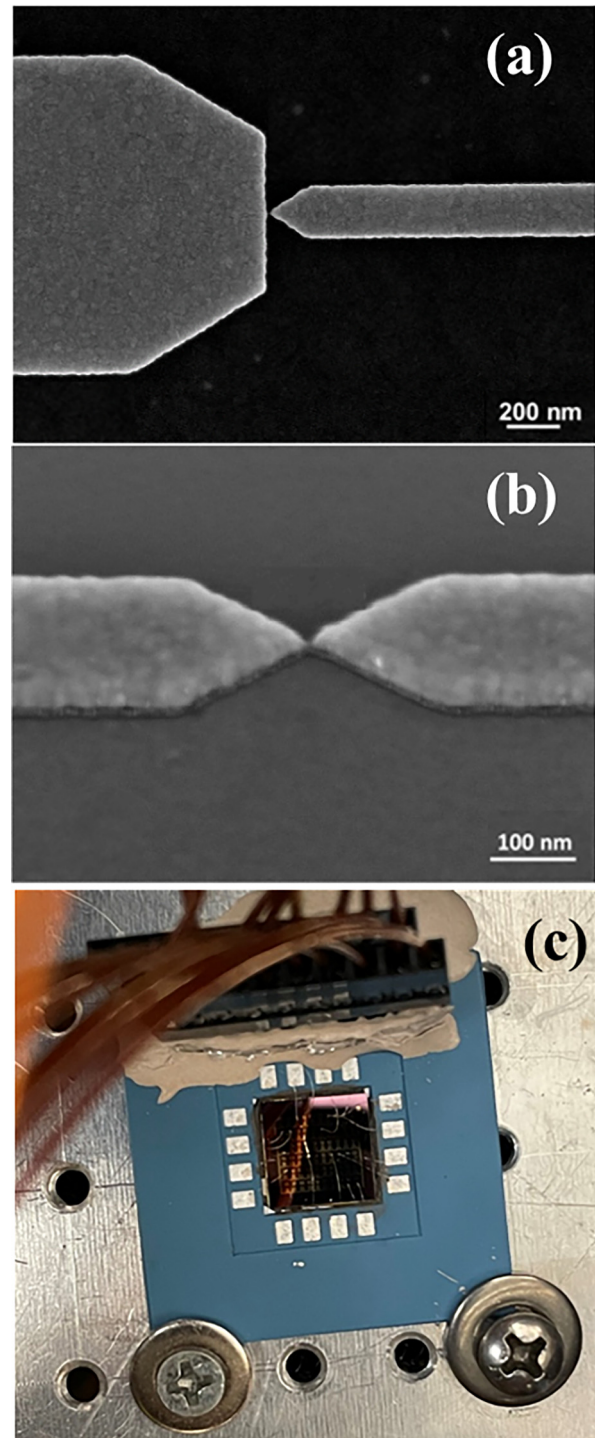


FIG. 1. (a) SEM images of the diode structure. (b) SEM image of the bowtie structure. (c) Image of a test die wire bonded to a LTCC test jig with multiple diode and bowtie structures. This jig is placed in the vacuum test chamber for characterization and lifetime testing.

the effect of different UV powers. The distance from the UV lamp to the center of the chamber is $\approx 6''$ where the sample was mounted. The tests were carried out at $\approx 7 \times 10^{-8}$ Torr. An Extorr Inc. XT100 residual gas analyzer was also used to monitor the partial pressure of the gas species inside the chamber. A Keysight B2902A source measurement unit was used as the voltage source as well as the current measurement device. The current was measured in real-time using a fixed step-up value where each step was 1.2 s.

For the long-term lifetime test, a separate test chamber was utilized. The lifetime test chamber is equipped with an ion pump, a turbomolecular pump, and a roughing pump, which maintains a high vacuum ($\approx 2.0 \times 10^{-9}$ Torr). The test setup consists of an aluminum plate where the test jig was attached. The lifetime test setup schematic is described elsewhere.¹⁵ The emitters were connected to the power supply through an electrical feedthrough using Kapton-coated wires which were attached to the jig. A fixed DC bias of 5 V was applied to the collector for the diode device and one of the emitters for the bowtie device for these lifetime experiments. The collector current data was logged with an interval of 1 min (real-time, no averaging) using a LabVIEW data acquisition system.

IV. EXPERIMENTAL RESULTS

A. Characterization of experimental results

Before and after UV irradiation, I-V sweeps were performed to find out the effect of UV light exposure on the gas desorption of planar devices and to evaluate the effects on the emission current. A 0–6 V DC sweep was applied to the collector with a step value of 0.06 V using a sweep time of 2 min.

I-V measurements for the bowtie device are shown in Fig. 2(a). First, an I-V sweep was performed while the UV light was off. The UV light was then switched on for 100 min, and an I-V sweep was carried out. 100 min of UV exposure was chosen based on our previous work^{19,25} where a significant improvement in emission current from Si-GFEA devices was observed. After each exposure, the UV light was switched off to remove the possibility of photoemission during I-V sweeps. The collector I-V curve after UV exposure is shown in Fig. 2(a). As can be seen in the graph, the collector current was ≈ 2.5 nA at 6 V before UV exposure and the collector current decreased to ≈ 1.8 nA at 6 V after 100 min of UV irradiation. It was observed that the decreased collector current remains constant with further sweeps. Also, the Fowler–Nordheim^{26,27} plot can be seen in Fig. 2(b) for the collector current which shows a much cleaner and linear plot after UV exposure, which indicates that most of the current is now likely from field emission. The collector current decrease can be attributed to the desorption of water vapor and possibly other adsorbates under UV irradiation.²⁸ The enhanced electron transport along the dielectric surfaces between the emitter and the collector can be attributed to adsorbates^{16,17,29} which consequently increase the surface leakage current. This effect was observed in our previous work³⁰ on vertical emitters. UV exposure removed the adsorbates, primarily water vapor, thus decreasing the leakage current. This decrease in the leakage current resulted in the reduction of the total collector current.

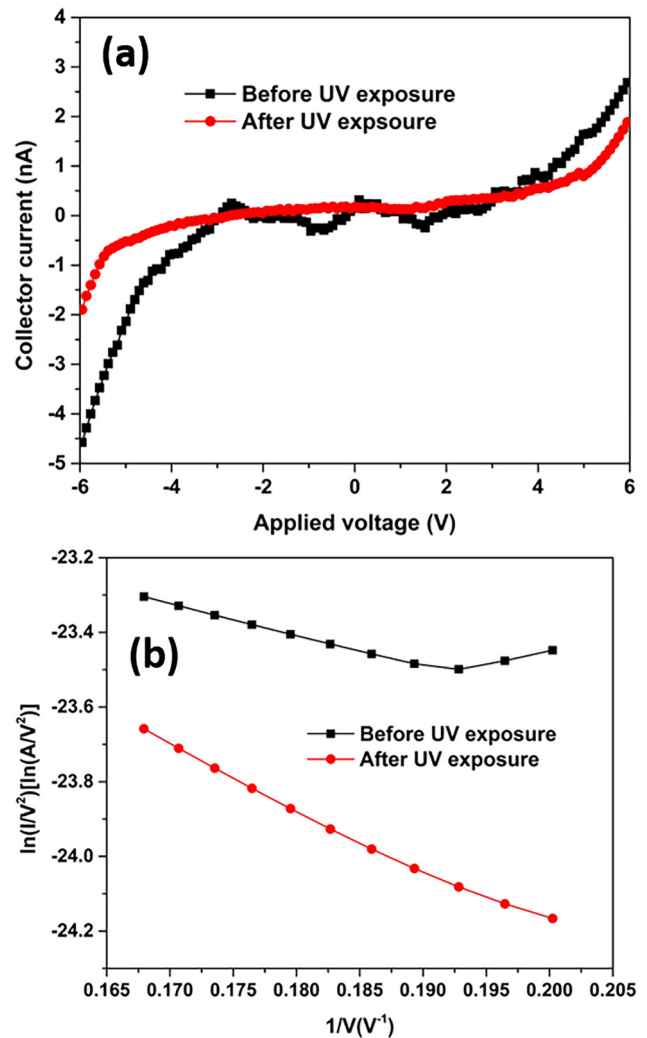


FIG. 2. Bowtie device. (a) I-V characteristics data before and after UV exposure and (b) corresponding F-N plot.

A similar phenomenon was observed for the diode device shown in Fig. 3(a), and the F-N plot can also be seen in Fig. 3(b). Like the bowtie device, the F-N plot for the diode device also shows a cleaner and more linear nature after UV exposure, which indicates that most of the current is likely from field emission. The before and after UV exposure collector current for the diode device is ≈ 5.4 and 3.2 nA, respectively, which again shows the reduction in current. The F-N plot for both the bowtie [Fig. 2(b)] and the diode device [Fig. 3(b)] shows a higher linearity after UV exposure. Also, from the F-N plots of both the devices, a_{FN} and b_{FN} were extracted,¹⁹ and the field enhancement factor (β) was calculated using the after-exposure F-N plots assuming that both tips were cleaned. A work function of 5.1 eV (Au)³¹ was used for the calculation of β for both devices. Then, these β were used to calculate the

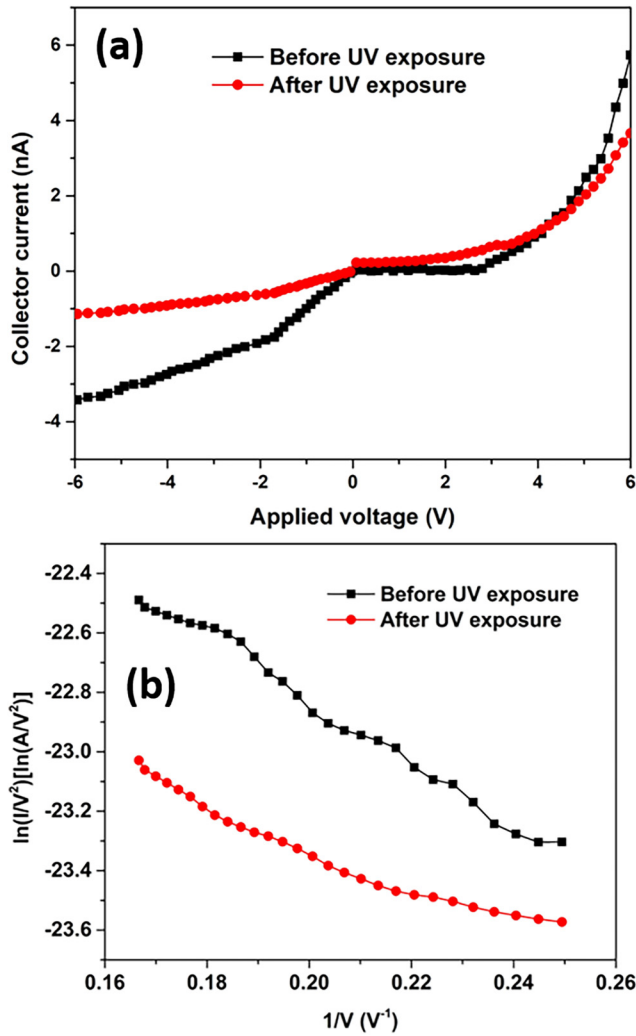


FIG. 3. Diode device. (a) I-V characteristics before and after UV exposure and (b) corresponding F-N plot.

work functions for before-exposure cases. The calculated work functions were 5.34 and 4.84 eV, respectively, for the bowtie and diode devices. These work functions do not match with the work function of Au, which suggests that the pre-exposure currents are not entirely field emission currents; thus, they do not follow the F-N or Murphy–Good model.^{27,32} In addition, while UV exposure should produce a cleaner (closer to Au) tip surface, the overall postexposure current was lower because the surface leakage current was greatly reduced.

After UV exposure, a cleaned tip could be attributed to this phenomenon. However, a reduction in the surface current and, consequently, a less leaky surface could also increase the linearity, where the larger portion of the measured current is due to field emission. To confirm the reduction of surface leakage, a reverse

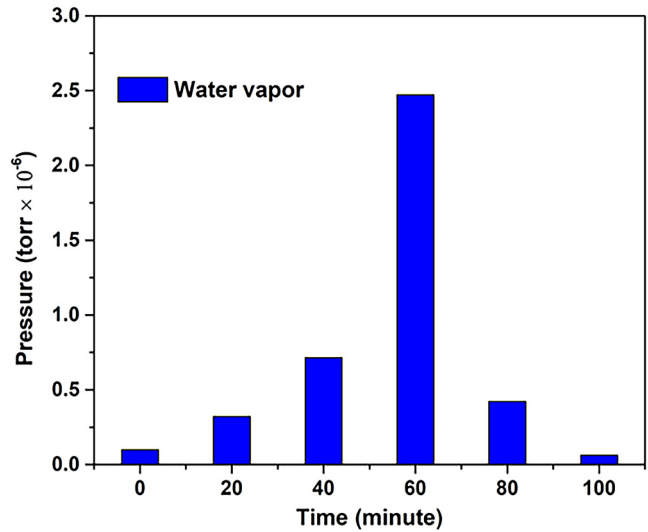


FIG. 4. Water vapor partial pressure vs UV exposure time taken using the RGA.

bias sweep was also applied to both the bowtie and diode devices, and the result can be seen in Figs. 2(a) and 3(a). From Fig. 2(a), it is observed that the collector current for the bowtie device under a reverse bias of -6 V was 4.5 nA before UV exposure and 2 nA after UV exposure. From Fig. 3(a), it is observed that the collector current for the diode device at a reverse bias of -6 V was 3.3 nA before UV exposure and 1 nA after UV exposure. These results demonstrate that a reduction in surface leakage occurs from UV exposure, resulting in reduced reverse bias current for the diode and reduced collector current for the bowtie.

Figure 4 shows water vapor desorption (measured using RGA) over time during UV exposure. From the plot, it can be observed that the desorption was maximum around 60 min. However, during the exposure, no I-V sweeps were carried out as water vapor was not sufficiently desorbed as can be seen in the plot.

B. After UV exposure long-term stability test results

Stability over time is one of the crucial characteristics of a field emitter electron source. In our previous work, we tested lateral emitters for up to ≈ 1400 h.¹⁵ These tests were performed without UV exposure.

The graph shows that the partial pressure for water vapor is the maximum around 60 min.

Also, in our prior work, we tested silicon-gated field emitters after UV exposure followed by several hours of air exposure.²⁵ From those sets of experiments, minimal degradation of emission current was observed for an air exposure of up to 6 h. From those experiments, it was concluded that those devices can be exposed to air for several hours (~ 6 h) without significant gas adsorption for transfer purposes. To check lateral emitter stability over time, the devices were transferred from the characterization test chamber to

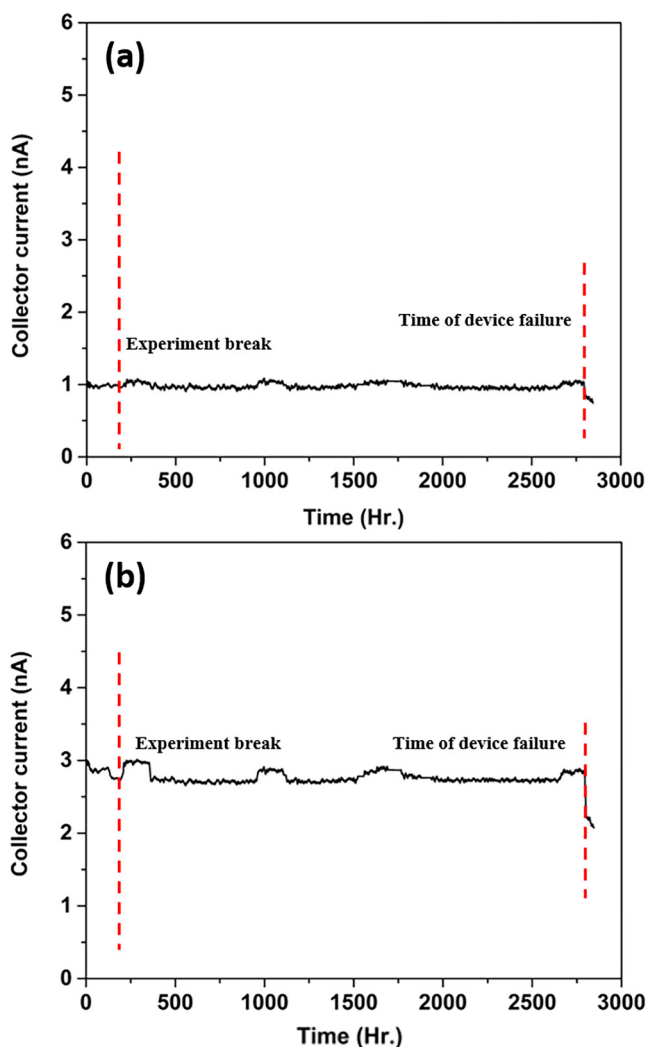


FIG. 5. Collector current vs time at five V_{DC} for (a) bowtie and (b) diode.

the lifetime test chamber right after UV cleaning and ran for over 2600 h at an applied constant DC voltage of 5 V. The long-term stability plot can be observed in Fig. 5 for both device structures.

Data was logged with a resolution of 1 min utilizing a LabVIEW code during the test. There was an experimental break (≈ 1 h) denoted by dotted red lines at around 250 h as shown in Figs. 5(a) and 5(b). A 25-point average filter was used on the raw data to comprehensively understand the variation of current over time. From the filtered (25 average) data, it can be observed that the bowtie and the diode were capable of emitting relatively constant field emission current over a time period of ≈ 2600 h with a current deviation of $<3\%$.

For the bowtie device [Fig. 5(a)], in spite of the fact that the device operated for more than 2600 h with a decrease of $<2\%$, the device ultimately failed at ≈ 2630 h, and a 25% drop in current was

observed. From Fig. 5(b), it can be observed that the diode device worked up to 2700 h with a deviation of $<3\%$, before failing, and a 28% drop in current was observed. Also, during the lifetime test, several current bumps can be observed for both devices. The reason is not understood.

C. Failure analysis

Both devices were removed after the lifetime test and examined under SEM. The SEM images for both structures are shown in Fig. 6.

In the case of the bowtie [Fig. 6(a)], the damage is located where the top layer (Au) is partially removed and the left tip appears to be partially damaged. In the case of the diode [Fig. 6(b)], the top layer (Au) is completely removed over both the collector and the tip. These phenomena could be attributed either to arc damage or thermal tip runaway.

The SEM images before and after experiments are of two different devices. SEM images of the mounted devices were not

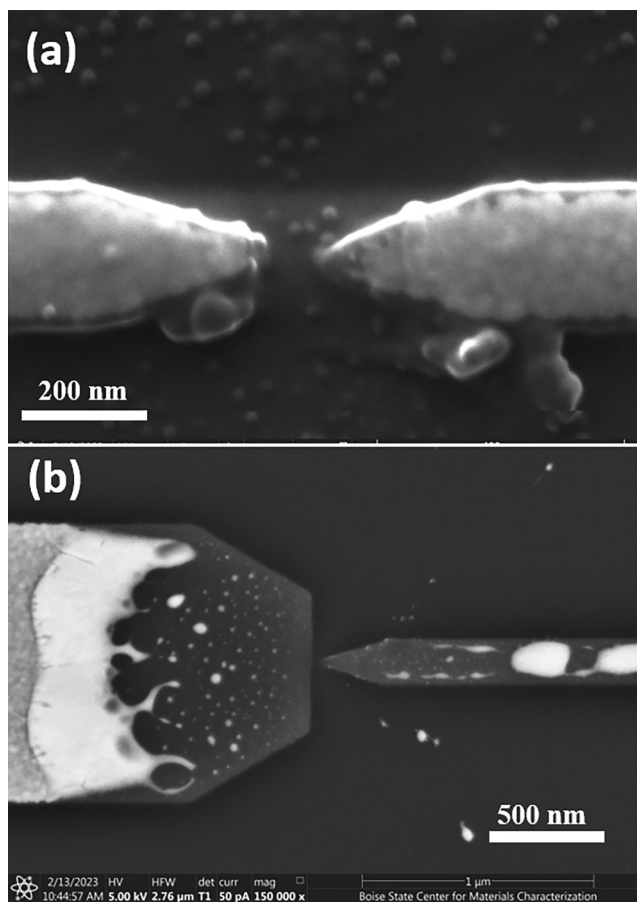


FIG. 6. (a) Bowtie structure. The top layer (Au) is partially removed and the left tip also seemed to be damaged. (b) Diode structure. The top layer (Au) is completely removed indicating melting. Only the bottom layer (Ti) can be seen.

practical on the wire-bonded structure. However, based on the field emission performances before failure, it can be assumed that the device structures were comparable to the devices shown in Fig. 1.

V. SUMMARY AND CONCLUSIONS

The bowtie and diode-type cold field emitters were studied for emission characteristics before and after UV exposure. The devices were also characterized for long-term current output stability (after UV exposure). From the I-V sweep, the observed collector current for the bowtie device, for an applied potential of 6 V was ≈ 2.5 nA and 1.8 nA before and after UV exposure, respectively. For the diode device, the observed collector current was ≈ 5.4 and 3.2 nA for before and after UV exposure, respectively. This reduction in current can be attributed to the removal of adsorbates (primarily, water vapor) from the surface, which reduces the surface leakage current. A reverse bias sweep also showed the reduction in collector current which was primarily surface leakage. A cleaner F-N plot after UV exposure also supports this conclusion. Prior research has clearly shown that UV desorbs water vapor as measured through RGA measurements. This surface leakage result is very important in understanding the emission from lateral-type devices. This result could also explain why lateral field emitter devices operated in air do not show a clear F-N plot; instead, most of the collector current could be due to surface leakage. A long-term stability study was also carried out on both devices after the exposure to UV light. It can be noted that the measured collector current is primarily the field emission current after UV exposure. It was observed that both the devices demonstrated stable field emission performance over a period of ≈ 2600 h with a current deviation of $< 3\%$. Failure occurred in both devices as confirmed by imaging. These field emitter devices demonstrated great possibility as electron sources for surface plasmon devices with femtosecond pulse³³ and NVCT devices, where a few nA of current with substantial stability over a long period of time is required. Additional devices for lifetime testing were not available. In the future, additional long-term stability studies on other devices, such as arrays of a bowtie or a diode will be carried out.

ACKNOWLEDGMENTS

Material support for this work was provided by the Air Force Office of Scientific Research under Grant No. FA9550-18-1-0436. The authors would also like to acknowledge undergraduate students Gerardo Herrera and Mason Cannon for their support. The authors would also like to acknowledge Boise State Center for Materials Characterization (BSCMC) for providing us help with the acquisition of the SEM images.

AUTHOR DECLARATIONS

Conflict of Interest

The authors have no conflicts to disclose.

Author Contributions

Ranajoy Bhattacharya: Formal analysis (equal); Investigation (equal); Methodology (equal); Validation (equal); Writing –

original draft (equal). **Marco Turchetti:** Resources (equal); Writing – review & editing (equal). **Matthew Yeung:** Resources (equal); Writing – review & editing (equal). **P. Donald Keathley:** Supervision (equal); Writing – review & editing (equal). **Karl K. Berggren:** Funding acquisition (equal); Supervision (equal). **Jim Browning:** Funding acquisition (equal); Supervision (equal); Validation (equal); Writing – review & editing (equal).

DATA AVAILABILITY

The data that support the findings of this study are available from the corresponding author upon reasonable request.

REFERENCES

- ¹T. Rybka, M. Ludwig, M. F. Schmalz, V. Knittel, D. Brida, and A. Leitenstorfer, *Nat. Photonics* **10**, 667 (2016).
- ²A. Kubo, K. Onda, H. Petek, Z. Sun, Y. S. Jung, and H. K. Kim, *Nano Lett.* **5**, 1123 (2005).
- ³W. P. Putnam, R. G. Hobbs, P. D. Keathley, K. K. Berggren, and F. X. Kärtner, *Nat. Phys.* **13**, 335 (2017).
- ⁴Y. Yang, M. Turchetti, P. Vasireddy, W. P. Putnam, O. Karnbach, A. Nardi, F. X. Kärtner, K. K. Berggren, and P. D. Keathley, *Nat. Commun.* **11**, 1 (2020).
- ⁵C. Karnetzky, P. Zimmermann, C. Trummer, C. Duque Sierra, M. Wörle, R. Kienberger, and A. Holleitner, *Nat. Commun.* **9**, 2471 (2018).
- ⁶H. Duyá Nguyen, J. Sang Kang, Man Li, and Yongjie Hu, *Nanoscale* **11**, 3129 (2019).
- ⁷J.-W. Han, D.-I. Moon, and M. Meyyappan, *Nano Lett.* **17**, 2146 (2017).
- ⁸W. P. Kang, J. L. Davidson, K. Subramanian, B. K. Choi, and K. F. Galloway, *IEEE Trans. Nucl. Sci.* **54**, 1061 (2007).
- ⁹R. Bhattacharya, N. Karaulac, W. Chern, A. I. Akinwande, and J. Browning, *J. Vac. Sci. Technol. B* **39**, 023201 (2021).
- ¹⁰H. H. Busta, J. E. Pogemiller, and B. J. Zimmerman, *J. Micromech. Microeng.* **3**, 49 (1993).
- ¹¹H. S. Uh, S. J. Kwon, and J. D. Lee, *J. Vac. Sci. Technol. B* **15**, 472 (1997).
- ¹²S.-H. Hsu, “Development of vertical nanodiamond vacuum field emission micro-electronic integrated devices,” Ph.D. dissertation (Vanderbilt University, 2014).
- ¹³R. Greene, H. Gray, and G. Campisi, “Vacuum integrated circuits,” in *1985 International Electron Devices Meeting*, Washington, DC, USA, 1-4 December, 1985 (IEDM, 1985), pp. 172–175.
- ¹⁴L. Zhang, A. Q. Gui, and W. N. Carr, *J. Micromech. Microeng.* **1**, 126 (1991).
- ¹⁵R. Bhattacharya, M. Turchetti, P. D. Keathley, K. K. Berggren, and J. Browning, *J. Vac. Sci. Technol., B* **39**, 053201 (2021).
- ¹⁶J. W. Osenbach, *Semicond. Sci. Technol.* **11**, 155 (1996).
- ¹⁷Y. Kayaba, K. Kohmura, and T. Kikkawa, *Jpn. J. Appl. Phys.* **47**, 8364 (2008).
- ¹⁸Y. Endo, I. Honjo, and S. Goto, *J. Vac. Sci. Technol. B* **16**, 3082 (1998).
- ¹⁹R. Bhattacharya, N. Karaulac, G. Rughoobur, W. Chern, A. I. Akinwande, and J. Browning, *J. Vac. Sci. Technol. B* **39**, 033201 (2021).
- ²⁰P. Danielson, U.S. patent US4660297A (28 April 1987).
- ²¹S. A. Guerrero, L. F. Velasquez-Garcia, and A. I. Akinwande, *IEEE Trans. Electron Devices* **59**, 2524 (2012).
- ²²M. Gilmore, N. E. McGruer, J. Browning, and W. J. Bintz, *Rev. Sci. Instrum.* **64**, 581 (1993).
- ²³J. Browning, N. E. McGruer, W. J. Bintz, and M. Gilmore, *IEEE Electron Device Lett.* **13**, 167 (1992).
- ²⁴S. Meassick, Z. Xia, C. Chan, and J. Browning, *J. Vac. Sci. Technol. B* **12**, 710 (1994).
- ²⁵R. Bhattacharya, M. Cannon, R. Bhattacharjee, G. Rughoobur, N. Karaulac, W. Chern, A. I. Akinwande, and J. Browning, *J. Vac. Sci. Technol. B* **40**, 010601 (2022).
- ²⁶R. H. Fowler and L. Nordheim, *Proc. R. Soc. London Ser. A* **119**, 173 (1928).
- ²⁷E. L. Murphy and R. H. Good, Jr., *Phys. Rev.* **102**, 1464 (1956).

- ²⁸H. D. Wanzenboeck, P. Roediger, G. Hochleitner, E. Bertagnolli, and W. Buehler, *J. Vac. Sci. Technol. A* **28**, 1413 (2010).
- ²⁹A. Di Bartolomeo, F. Giubileo, L. Iemmo, F. Romeo, S. Russo, S. Unal, M. Passacantando, V. Grossi, and A. M. Cucolo, *Appl. Phys. Lett.* **109**, 023510 (2016).
- ³⁰R. Bhattacharya, N. Karaulac, W. Chern, A. I. Akinwande, and J. Browning, "Temperature effects on gated silicon field emission array performance," *J. Vac. Sci. Technol. B* **39**(2), 023201 (2021).
- ³¹M. Turchetti, Y. Yang, M. Bionta, A. Nardi, L. Daniel, K. K. Berggren, and P. D. Keathley, *IEEE Trans. Electron Devices* **69**, 3953 (2022).
- ³²R. G. Forbes, *Mod. Dev. Vac. Electron Sources* **135**, 387 (2020).
- ³³M. R. Bionta, F. Ritzkowsky, M. Turchetti, Y. Yang, D. Cattozzo Mor, W. P. Putnam, F. X. Kärtner, K. K. Berggren, and P. D. Keathley, *Nat. Photonics* **15**, 456 (2021).